REPORT DOCUMENTATION PAGE

AFRL-SR-BL-TR-00-

01605

1. AGENCY USE ONLY *(Leave blank)*	2. REPORT DATE	3. REPORT TYPE AND DATES COVERED
		Final 15 Mar 96 to 14 Mar 99

4. TITLE AND SUBTITLE
Experimental Study of Coulomb Crystallization in Dusty Plasma

5. FUNDING NUMBERS
61102F
2301/EX

6. AUTHOR(S)
Dr Rahman

7. PERFORMING ORGANIZATION NAME(S) AND ADDRESS(ES)
University of California, Riverside
B132 Library South
Riverside CA 92521-0217

8. PERFORMING ORGANIZATION REPORT NUMBER

9. SPONSORING/MONITORING AGENCY NAME(S) AND ADDRESS(ES)
AFOSR/NE
801 N Randolph Street Rm 732
Arlington, VA 22203-1977

10. SPONSORING/MONITORING AGENCY REPORT NUMBER
F49620-96-1-0113

11. SUPPLEMENTARY NOTES

12a. DISTRIBUTION AVAILABILITY STATEMENT
APPROVAL FOR PUBLIC RELEASE, DISTRIBUTION UNLIMITED

12b. DISTRIBUTION CODE

13. ABSTRACT *(Maximum 200 words)*

In this project we studied the lattice structure of dusty plasma Coulomb crystls formed in rectangular conductive grooves as a function of plasma temperature and density. The crystal appears to be made of mutually repulsive columns of grains confined by the walls of the groove. The columns are oriented along the direction of the electrode sheath electric field.

20000503 101

14. SUBJECT TERMS

15. NUMBER OF PAGES

16. PRICE CODE

17. SECURITY CLASSIFICATION OF REPORT	18. SECURITY CLASSIFICATION OF THIS PAGE	19. SECURITY CLASSIFICATION OF ABSTRACT	20. LIMITATION OF ABSTRACT
UNCLASSIFIED	UNCLASSIFIED	UNCLASSIFIED	UL

PROJECT FINAL REPORT

TITLE: EXPERIMENTAL STUDY OF COULOMB CRYSTALIZATION IN DUSTY PLASMA

GRANT NO.: F49620-96-1-0113

PRINCIPAL INVESTIGATOR: DR. HAFIZ-UR-RAHMAN

DURATION: 15 MARCH 96 - 15 MARCH 99

PROGRAM MANAGER: DR. ROBERT J. BARKER

1. Introduction

In this project we studied the lattice structure of dusty plasma Coulomb crystals formed in rectangular conductive grooves as a function of plasma temperature and density. The crystal appears to be made of mutually repulsive columns of grains confined by the walls of the groove. The columns are oriented along the direction of the electrode sheath electric field. A simple phenomenological model wherein the inter-grain spacing results from an attractive electric field induced dipole-dipole force balanced by a repulsive monopole Coulomb force is consistent with observed features of the Coulomb crystal. The importance and pioneering nature of the work has been recognized by a publication in *Physical Review Letters* [1]. An *invited talk* a the last American Physical Society, Division of Plasma Physics Meeting held last year also resulted from the work [2]. Another oral presentation on the research was done at the "Dusty Plasma Workshop" in Boulder Co in April 1998 [3]. An additional experimental paper has also been published [4]. Two theoretical papers have also resulted from this research and have been published in peer reviewed journals [5,6].

Our major technical accomplishments are:

- developed sensitive and reproducible techniques to measure the plasma temperature and density
- made accurate measurements of the intergrain spacing in the Coulomb crystal as a function of the plasma parameters
- developed a model to understand the inter-grain coupling in the horizontal and vertical directions for the dust particles in the Coulomb crystal.
- studied the chemical composition and crystal structure of the SiO_2 grains formed in the plasma
- made preliminary measurements on the charge of individual dust grains
- made accurate measurements of the grain vibration and rotation frequency.
- attempted a theoretical understanding of the vibration and rotation dynamics of the grains in terms of their structure, charges and dipole moments. This was done in collaboration with our colleagures at UCSD.
- performed preliminary experiments on positively charge dusty plasma Coulomb crystal formation with the use of UV light ionization of the dust grains.

2. BACKGROUND

A dusty plasma can be loosely defined as an ionized gas with dispersed charged solid particulates, or dust grains, of micron to sub-micron sizes. The physics of dusty plasmas in space environments, such as planetary atmospheres and rings, comets, and the interstellar and interplanetary media, have been studied for some time [e.g. 7-11]. Recently there has been much interest in the physics of dust in plasma processing devices, used in the microelectronics industry, primarily due to the defects in

microelectronic circuits caused by dust contamination [e.g. 12-13]. Important new developments in laboratory dusty plasmas involve experiments demonstrating the formation of Coulomb lattices or crystals of charged dust grains in a plasma, the so-called "plasma crystals" [14-17]. As suggested by Ikezi [18], negatively charged dust grains (due to the higher mobility of the electrons) in a plasma can form Coulomb crystals when their Coulomb intergrain potential energy is sufficiently larger than their thermal energy. This condition is $\Gamma_d = \frac{e^2 Z_d^2}{dT_d} \exp(-d/\lambda_D) > \Gamma_{dc}$, where Z_d is the dust charge state, d is the inter-grain spacing, T_d is the dust grain thermal energy, λ_D is the plasma Debye length and Γ_{dc} is some critical value which is approximately 170 for a one component plasma [18]. The exponential factor accounts for screening of the dust charge by the background plasma.

In Coulomb crystal experiments, the grains are confined in the sheaths of the electrode configurations. In the vertical direction the grains are levitated by the electrostatic force associated with the electric field in the sheath, while the monopole (Coulomb) repulsion between the grains keeps the spacings between the layers. In the horizontal direction, the grains are also confined by the force associated with the horizontal component of the electric field in the sheath associated with the particular electrode configuration. It has also been conjectured that there may be mechanisms which lead to additional attractive forces between the grains that may influence the lattice structure [e.g. 19-21]. Here we report on a new regime of dust Coulomb crystals, where the grain sizes are on the order of ~ 50μm (larger than those in previous Coulomb crystal experiments), and

where there appears to be a strong inter-grain attractive coupling which leads to the formation of distinct grain columns along the sheath electric field. We attribute this to an electric field induced dipole-dipole interaction between the grains. This possibility has been proposed recently by an analysis of the phase diagram of such crystals [22]. We first give experimental results and then discuss our phenomenological model.

3. TECHNICAL PROGRESS

The experimental setup at UCR used for the generation of the Coulomb crystal is shown in figure 1. A 10cm diameter Pyrex 4-way cross was used as the reaction chamber. Inside, 5cm x 7.5cm Aluminum electrodes were arranged 5cm apart in the form of a capacitor. The bottom electrode has a 1cm deep, 4cm wide, 7.5cm long groove in the middle. The Aluminum electrodes were coated with black conductive paint to minimize light scattering off the electrode. The front end of the groove was made of a conductive and transparent Indium Tin Oxide (ITO) coated glass to facilitate easy observation of the Coulomb crystal from that direction. The rear end of the groove was capped with copper foil. A 100 turn 10cm diameter Helmholtz coil is added to the chamber to generate a 50 gauss magnetic field which confines the plasma and leads to the efficient production of large particles during the growth process.

First the chamber was pumped below 1 mTorr and Ar gas was leaked into the chamber to a pressure of 60mTorr. A 5 amp current was then supplied to the Helmholtz coils. A stable plasma was next formed by supplying 15 W forward rf power at 34 MHz to the electrodes. SiH_4 and O_2 gas (about 20mTorr of each) were then introduced into the

chamber and allowed to react. The gases were shut off after 15 seconds. The reaction leads to the nucleation of SiO_2 crystallites. The SiO_2 grains grew in size by aggregation. The magnetic field was turned off at the end of the growth process (about three minutes). This led to a relatively homogenous distribution of grain sizes. Scanning electron microscope image of a typical grain is shown in figure 2. The grains appear to be porous aggregates of 100nm sized hexagonal crystallites. The typical grain had a irregular rod-like shape about 100-140 microns long and 40-60 microns in diameter.

The Ar pressure was raised to 150mTorr at the end of the grain growth cycle. A 20mW 640nm diode laser was directed into the electrode groove for the observation of the grains. The laser light scattered off the dust grains is used to visually identify their position. The dust grains condense into a geometric pattern a few minutes after the increase in Ar pressure. Top view images (with the help of a mirror held at 45^{o} to the plane of the electrode) and side view images (through the conductive ITO coated glass plate) were taken with a CCD camera and recorded on magnetic tape for analysis.

The lattice structure of the plasma crystal was studied as a function of forward rf power. Top view and side view images are shown in Figure 3a and b respectively. Figure 3a is a top view of a typical hexagonal array formed at low forward rf powers below 2W. As the power is increased the crystal loses its horizontal structure and breaks up into distinct vertical columns of grains as shown in Figure 3b. The bottom of the electrode groove corresponds to the horizontal bright streak at the bottom of the picture (caused by the laser light scattering off the groove bottom). The left (right) edge of the picture corresponds to the center (right sidewall) of the groove. The columns were observed to be

robust; moving and interacting as single entities. Collisions between columns appear to be elastic and repulsive. This points to a screened repulsive interaction between columns. The columns remain intact even after collision. The robustness of the column suggests a strong attractive coupling between the grains of the column. More insight can be gained by noting the orientation of the columns in figure 3b. While the columns near the center of the groove (left of picture) are vertical, those near the side wall (right of picture) are tilted, with the tilt increasing with decreasing distance to the side wall. The columns thus appear to be oriented parallel to the sheath electric field.

The inter-grain spacing along the columns as a function of the forward rf power is shown in Figure 4. The thermal energy of the dust grains results in a distribution of inter-grain spacings. The solid square represents the average spacing measured and the limits on the error bar correspond to the maximum and minimum spacing measured at a given forward rf power. The inter-grain spacing is observed to decrease rapidly with increasing forward rf power till 4W and more gradually at higher powers.

The plasma temperature and density were measured using a Langmuir type single probe. A 0.5mm diameter tantalum wire in a 0.63 cm ceramic sleeve was used. A 3mm long section of the probe was exposed outside the sleeve and placed 1cm above the bottom electrode. As dust contaminated the probe the measurements were done in a dust free plasma at the same Ar pressure. The temperature of the plasma was calculated from the slopes of the *I-V* characterstics near the zero-current point [19]. The electron temperature (T_e) so derived is plotted along the left axis in figure 5 (dark squares). The range of

temperatures shown by the error bars correspond to measurements ±2V around the zero-current point. T_e is seen to increase until 4W rf forward power and thereafter saturate around 10 eV. Increase in the forward rf power beyond 4W results in increased density and volume of the plasma.

The ion saturation current was used to calculate the plasma density n [19], which is plotted as open circles along the right axis in figure 5. The error bars correspond to the error limits in the measurement of T_e. The density is observed to increase with increasing rf power. The debye length (λ_D) given by $\lambda_D = (T_e/4\pi ne^2)^{1/2}$ corresponding to the measured temperatures and electron densities, decreases from 0.8mm to 0.4mm for forward rf powers between 1W and 10W respectively. This corresponds well to the decrease of inter-grain spacing (figure 4), consistent with the assumption that the screened monopole Coulomb interaction plays a dominant role in the inter-grain spacing.

We use a simple phenomenological model that appears to be consistent with the observations. From the experimental observations, there appear to be at least four main interactions that affect the formation of the Coulomb crystal in this experiment with large grains of radius ~50μm. These include (1) the electrostatic force due to the electric field in the sheath in the groove, (2) gravity, (3) the screened monopole repulsive interaction between the negatively charged grains, and (4) an attractive electric field induced dipole interaction (the ion drag force, though in the same direction as gravity, is smaller, and is neglected). Foremost, the grains are levitated inside the electrode groove by the electrostatic force due to the sheath electric field E_0 . Thus $eZ_d E_0 = m_d g$, where

m_d is the dust mass ($m_d = (4\pi/3)\rho_d a^3$, where a is the grain radius and ρ_d is the grain mass density) and g is the acceleration due to gravity. Also $-eZ_d \sim a\phi_s$ for a negatively charged 'isolated' grain (here ϕ_s is the grain surface potential). The sheath electric field can induce a polarization on the dust grains with a dipole moment P ($= E_0\, a^3$). The attractive dipole-dipole force between aligned dipoles separated by a distance d, taking into account screening by the background plasma, is given by [22]:

$$F_{dd} = \frac{6P^2}{d^4}\left(1 + x + \frac{1}{2}x^2 + \frac{1}{6}x^3\right)\exp(-x) \qquad (1)$$

where $x = d/\lambda_D$. Comparing this force with the screened monopole repulsion between the negatively charged dust grains given by

$$F_{mm} = \frac{Z_d^2 e^2}{d^2}(1+x)\exp(-x) \qquad (2)$$

we estimate that $F_{dd}/F_{mm} \sim 6 \times 10^{-6}(a/d)^2\, a^6\, \phi_s^{-4}$, neglecting screening (here a and d are in microns, ϕ_s is in Volts and ρ_d=2.6g/cm^3). Thus F_{dd}/F_{mm} scales strongly with grain radius (propotional to a^8) within our approximation and can be of the order of unity for parameters of this experiment with large grain sizes.

Balancing F_{mm}=F_{dd} gives a rough equilibrium inter-grain lattice spacing d for given plasma conditions represented by plasma (electron) temperature T_e (assuming $e|\phi_s| \sim T_e$) and plasma density n. This equilibrium spacing d derived from the above model is plotted as a function of the forward rf power as a solid line in figure 4. The values of T_e from the best fit curve of figure 5 were used. When screening is neglected (i.e., x=0) the best fit corresponds to spherical grains of radius $a \approx 64\,\mu$m. If one includes screening,

while noting that $x \approx 2$ for the entire range of rf power, then $a \approx 58\,\mu m$ for the best fit. In both cases the porosity of the grains was neglected i.e. ρ_d=2.6g/cm^{-3}. These values for the grain radius are consitent with the measured values (see figure 2). There is good agreement between the dipole-dipole interaction model and the observed dependence of the inter-grain spacing with forward rf power. The grain dipole moment will lead to the observed orientation of the columns parallel to the sheath electric field.

We note that the electric field induced dipole interaction has been discussed in relation to dust plasma crystals [22] and to lattices of colloids in dilute suspension [e.g. 24-26]. For example, charged collodial grains can aggregate into chain structures under the influence of a screened Coulomb repulsive force and an electric field induced dipole attraction [26]. We also note that other mechanisms for attractive interactions between grains in Coulomb crystals have been suggested. For example, the asymetry of charge between the leading and trailing hemispheres of a dielectric grain in a flowing plasma can lead to a dipole moment of the grains, and this may lead to an attractive dipole-dipole force [27,28]. It has also been suggested that an attractive force between grains may arise due to a polarization of the Debye sheath around the grain by an external electric field (and associated density gradients) [29]. Another suggestion involves the focusing of ions flowing in the sheath due to deflection of ion orbits by the highly negatively charged grains which too leads to an attractive force [19]. Yet another suggestion involves wake potential effects in a plasma [20,21], which result in an attractive force between neighboring grains in the direction of flow. While these suggestions have yet to be tested and may not even be mutually exclusive with one another or with the model proposed in

the present paper, it appears that the attractive electric-field induced dipole interaction model is consistent with the present experimental results in the regime of large grain size. Finally we developed experiments to create positively charged dust grain Coulomb crystal. Here we used UV light from a Deuterium lamp to ionize 0.5micron diameter CeO_2 dust grains. First a vacuum chamber similar to the one used in the above experiments was developed. A delivery system to sprinkle the CeO_2 dust grains inside the vacuum chamber was incorporated into the vacuum chamber. A sapphire window which UV transparent was used to transmit the UV light from the Deuterium lamp. We verified the photoionization of the dustgrains by looking for the drift of the grains in a static electric field. The static electric field was applied with the aid of a parallel plate capacitor. However the intensity of the UV lamp appeared insufficient to ionize the dust grains to the 10^5e charge that would be necessary for the formation of positively charged dust grain Coulomb crystal.

5. Conclusion

In conclusion, we have measured the lattice structure and inter-grain spacing of Coulomb crystals formed in rectangular conductive grooves as a function of plasma temperature and density. From the dynamics of the grains, the Coulomb crystal appears to be made of mutually repulsive columns of grains oriented along the sheath electric field and confined by the the walls of the electrode groove. The main features of our experiment can be explained by a phenomenological model where the inter-grain coupling along the column is determined by a balance between an attractive electric field induced dipole-dipole and a repulsive monopole interaction between the charged grains. We also developed experiments to form a positively charged dust grain Coulomb crystal. However the

intensity of the UV light was insufficient to cause highly charged grains. UV lasers such as a N_2 laser might be necessary for the formation of positive dust Coulomb crystals.

BIBLIOGRAPHY

[1]. U. Mohideen, H.U. Rahman, M. A. Smith, M. Rosenberg and D. A. Mendis, "Inter-grain coupling in dusty plasma Coulomb crystals,' Phys. Rev. Lett., **81**, p. 349 (1998).

[2]. U. Mohideen, H.U Rahman, M. A. Smith, M. Rosenberg, and D.A. Mendis, "Inter-grain coupling in dusty plasma Coulomb crystals," APS DPP Meeting 1999, (Invited talk); Bull. Of APS , **44**, 169 (1999).

[3]. U. Mohideen, H. U. Rahman, M. A. Smith, M. Rosenberg, and D.A. Mendis, " Inter-grain coupling in dusty plasma Coulomb crystals, Workshop on Dusty Plasmas, Boulder, Co, 1998. Invited Talk.

[4]. M.A. Smith, H.U. Rahman and U. Mohideen, "Dusty plasma crystals: Effect of electrode geometry," in "Dusty Plasma Crystals," Edited by A.D. Mendis and P.K. Shukla, World Scientific Press, Singapore (1997).

[5]. P.K. Shukla and H. U. Rahman, "Instability of electrostatic dust-cyclotron waves and associated wake potential," Planet. Space Sci., **46**, p. 541 (1998).

[6]. P.K. Shukla and H.U. Rahman, "Low frequency electromagnetic waves in uniform gravitating dusty magnetoplasmas," Planet. Space. Sci., **44**, p. 469 (1996).

[7]. E.C. Whipple, Jr., *Rep. Prog. Phys.* **44**, 1197 (1981).

[8]. C. K. Goertz, *Rev. Geophys.* **27**, 271 (1989).

[9]. D. A. Mendis and M. Rosenberg, *Annu. Rev. Astron. Astrophys.* **32**, 419 (1994).

[10]. M. Horanyi, *Annu. Rev. Astron. Astrophys.* **34**, 383 (1996).

[11]. T. W. Hartquist, W. Pilipp, and O. Havnes, *Astrophys. Space Sci.* **246**, 243 (1997).

[12]. G. S. Selwyn, *Jpn. J. Appl. Phys.* **32**, 3068 (1993).

[13]. A. Bouchele, *Physics World* **6**, 47 (1993).

[14]. H. Thomas, G.E. Morfill, V. Demmel, J. Goree, B. Feuerbacher, and D. Mohlmann, *Phys. Rev. Lett.* **73**, 652 (1994).

[15]. J. H. Chu and Lin I, *Physica A* **205**, 183 (1994); *Phys. Rev. Lett.* **72**, 4009 (1994).

[16]. Y. Hayashi and K. Tachibana, *Jpn. J. Appl. Phys.* **33**, L814 (1994).

[17]. A. Melzer, T. Trottenberg, and A. Piel, *Phys. Lett.* A **191**, 301 (1994).

[18]. H. Ikezi, *Phys. Fluids* **29**, 1974 (1986).

[19]. F. Melandso and J. Goree, *J. Vac. Sci. Technol.* A **14**, 511 (1996).

[20]. S. V. Vladimirov and M. Nambu, *Phys. Rev.* E **52**, 2172 (1995).

[21]. M. Nambu, S.V. Vladimirov, and P.K. Shukla, *Phys. Lett* A **203**, 40 (1995).

[22]. H.C. Lee, D.Y. Chen and R. Rosenstein, Phys. Rev. E, **56**, 4596 (1997).

[23]. I. H. Hutchinson, "The principles of plasma diagnostics," Cambridge Univ. Press, New York (1987).

[24]. R. E. Kusner, J. A. Mann, J. Kerins, and A. J. Dahm, *Phys. Rev. Lett.* **73**, 3113 1994).

[25]. Q. Lei, X. Lei, C. Zhou, and N. Ming, *Phys. Rev.* E **51**, 1586 (1995).

[26]. P. A. Adriani and A. P. Gast, *Faraday Discuss. Chem. Soc.* **90**, 17 (1990).

[27]. G. Lapenta, *Phys. Rev. Lett.* **75**, 4409 (1995).

[28]. J. W. Manweiler, T. P. Armstrong, and T. E. Cravens, in *The Physics of Dusty Plasmas*, (ed. P.K. Shukla et al.), World Scientific, p. 22 (1996).

[29]. S. Hamaguchi and R. T. Farouki, *Phys. Rev.* E **49**, 4430 (1994).

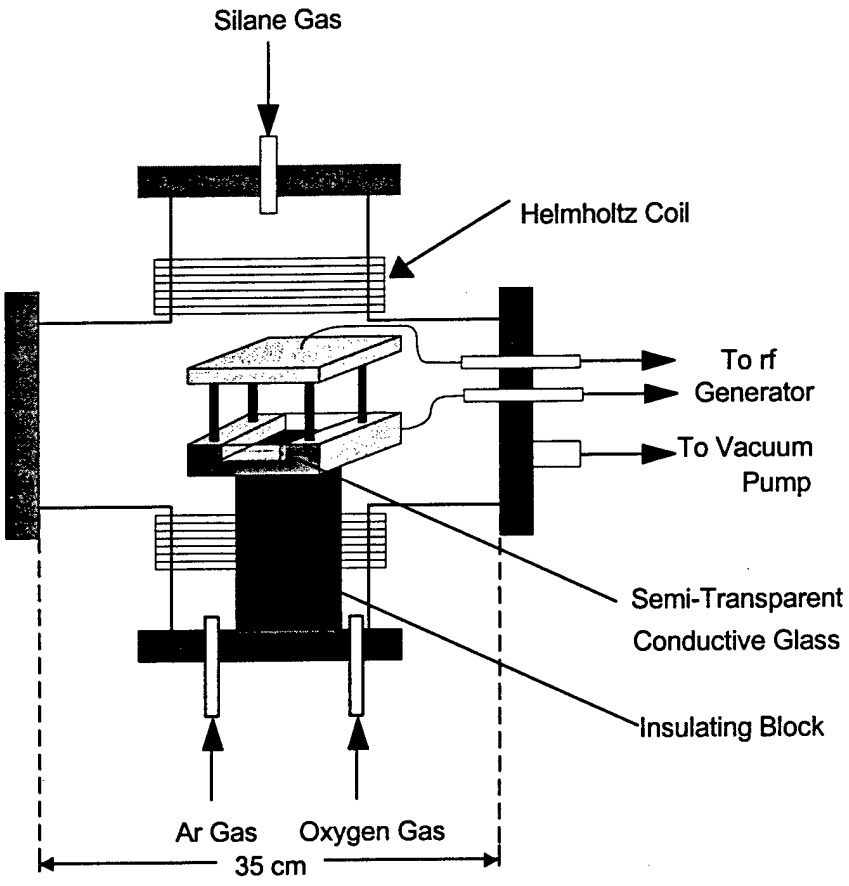

Figure 1: The experimental setup used for dusty plasma Coulomb crystal generation

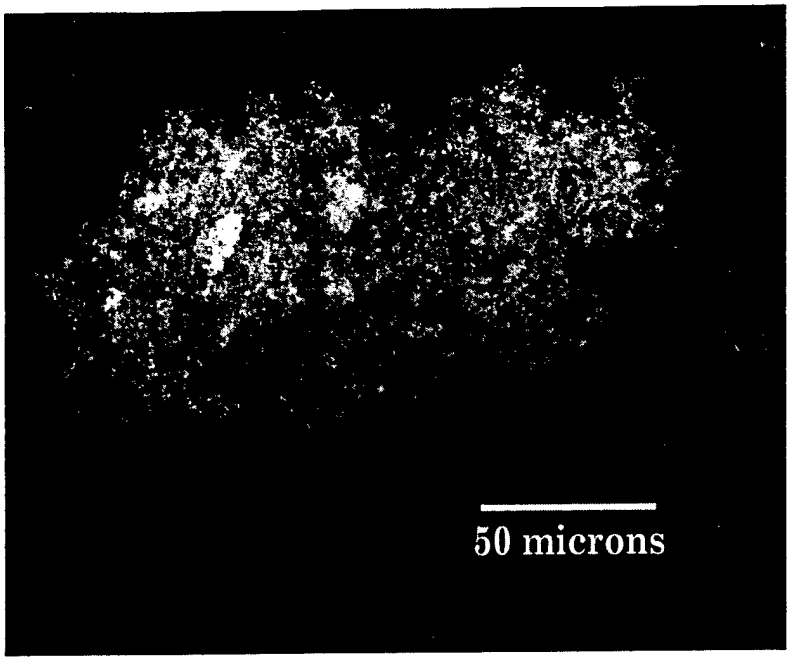

Figure 2: Scanning electron micrograph of a dust grain formed during the growth process.

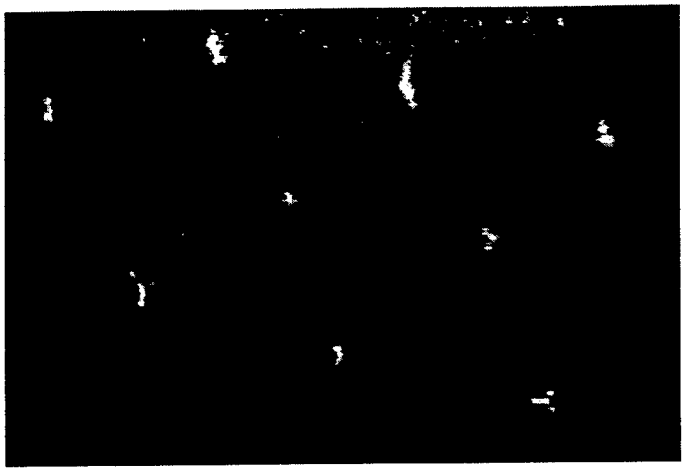

(a)

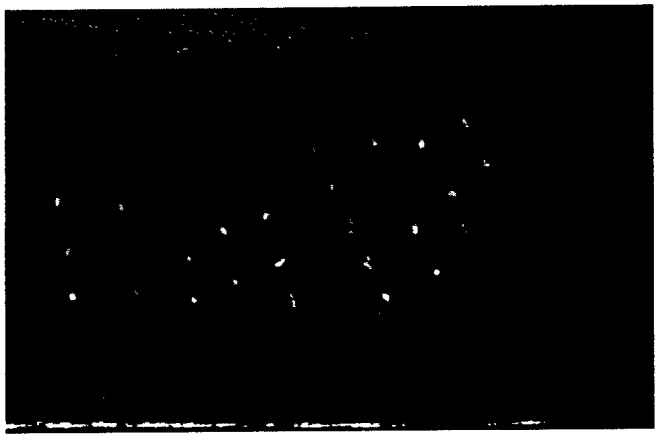

(b)

Figure 3: (a) Top view of hexagonal array formed at forward rf powers below 2W. (b) Side view image of the Coulomb crystal at large forward rf power taken through the transparent front electrode. The left (right) edge of the picture corresponds to the center (right sidewall) of the groove. The bright streak across the bottom of the picture corresponds to the groove bottom.

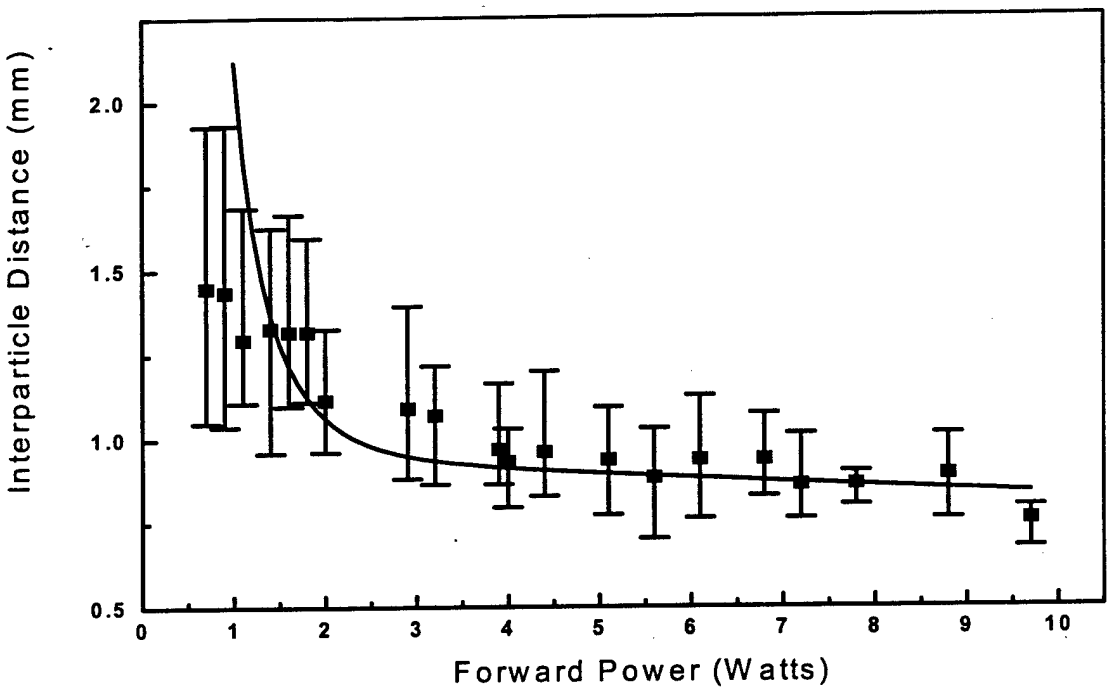

Figure 4: The inter-grain spacing d along the columns measured as a function of the forward rf power. The solid line is the predicted behavior of the phenomenological model with x=0 for spherical grains of radius $a \approx 64\ \mu m$.

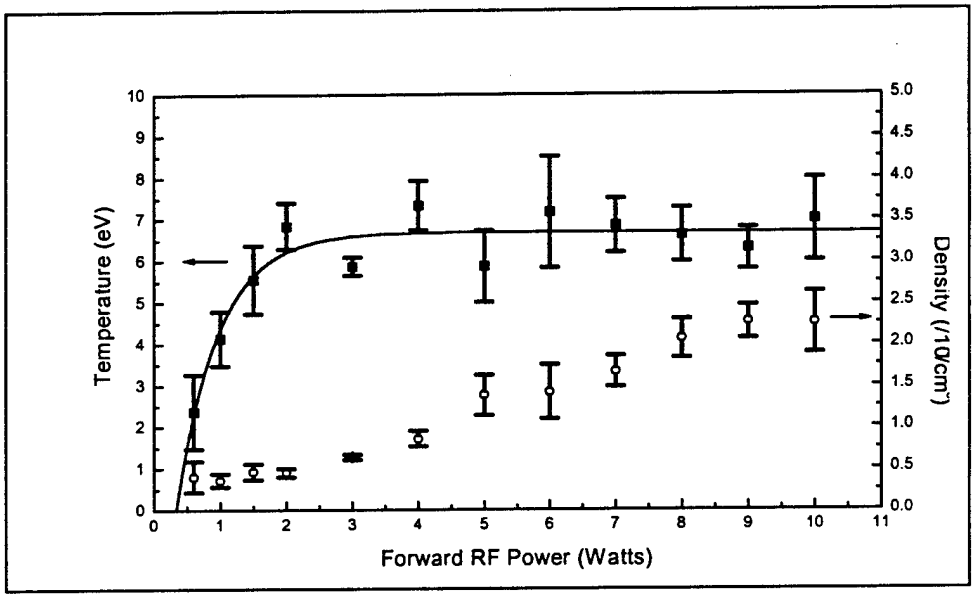

Figure 5: The average plasma electron temperature (left axis) as dark squares and density (right axis) as open circles plotted as function of the forward rf power. Solid line is a best fit to temperature data.